Model and Dynamical Analysis of a Tattooing Device

Filip SARBINOWSKI
Department of Applied Mechanics, Poznan University of Technology
Jana Pawła II 24, 60-965 Poznan, filip.j.sarbinowski@doctorate.put.poznan.pl

Roman STAROSTA
Department of Applied Mechanics, Poznan University of Technology
Jana Pawła II 24, 60-965 Poznan, roman.starosta@put.poznan.pl

Abstract

The paper presents the physical model of the tattooing device. The model is described by three degrees of freedom and a series of linear and nonlinear dynamic parameters and excitation, whose values are determined – depending on the available data and resources – by analytical, numerical and experimental methods. There are also presented a solution of motion equations and the assessment of the impact of individual parameters on the nature of solutions, and moreover, it is indicated a modification of the structure, the use of which results in decrease the amplitudes of the body structure vibrations.

Keywords: Nonlinear dynamics, vibrations, design optimization, tattoo

1. Introduction

In the last few years, we can observe the dynamic expansion of tattooing [1]. This art, that is known since the age of primitive civilization [2], has in recent years become a way to decorate the body and the manifest of opinions used by people from all social groups, therefore, the requirements for tattoo machines are growing in a natural way [3].

One of the key features affecting the comfort and quality of the tattooing process is the dynamics of the tattoo device - a small vibrations provides a steady grip and stable work [4]. Despite this rather obvious thesis, among the scientific studies it is in vain to look for works on this subject. The reasons for this state should be found in the fact that people related to art of tattooing usually do not have specialized knowledge in the field of machine dynamics, for scientists, however, this issue may seem trivial and not worth the attention. A closer look at the problems, however, shows that – due to the construction of such devices and the nature of their work – many nonlinear parameters may appear in the design, and these may be the cause of interesting phenomena [5]. Market review in search of prices of machines characterized by reduced vibrations [6], also allows to conclude that such research has not only a large cognitive but also commercial potential.

The two types of tattooing machines are commonly used – coil and rotary. The second ones are characterized by a more complex kinematics and thus a larger number of parameters that should be considered during the analysis, therefore these are the subject of this paper.

2. Subject of study – construction model

In this work, the vertical vibrations of Colibri 13 tattoo machine were analyzed (Fig. 1).

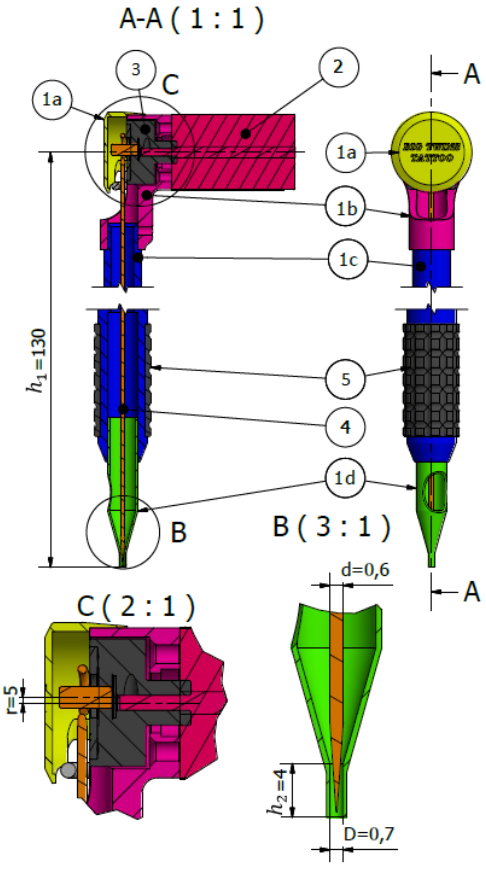

Figure 1. Device construction

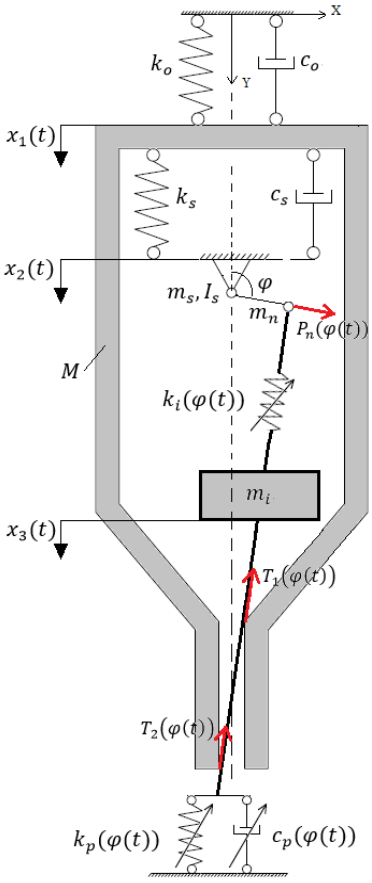

Figure 2. Device model

The main element of the device is a four-part body made of aluminum alloy (1.1a–d). The motor (1.2) connected to the body is connected to the eccentric system (1.3), which forces vertical movements of the steel needle in the range of ± r (1.4). In addition, a rubber spacer (1.5) is placed on the body to increase the grip of the operator.

The real construction has been reduced to a discrete model with three degrees of freedom, shown in Fig. 2. Interaction between the body of the machine with mass $M = 32$ g and the operator was approximated by the spring k_o and damper c_o. The value of coefficient of elasticity k_o was determined on the basis of FEM analyzes in the ANSYS environment. In the program a model consisting of two parts has been defined: a pin simulating a housing and attached to it, fixed on the external surface sleeve – the operator's

hand, which was given hyperelastic properties on the basis of [7]. The pin was loaded with axial force increasing in six consecutive steps from 0 to 1.5 N and in each of them the axial displacement of the spindle corresponding to the body deflections from the equilibrium position $x_1(t)$ was recorded. The diagram of the dependence of force on displacement and the resultant dependence of the stiffness and displacement coefficient is shown in Fig. 3. Damping here is more difficult than strictly define – to perform a simulation analogous to that concerning stiffness, the knowledge of skin Rayleigh coefficients or damping ratio would be required. On the basis of the organoleptic analysis, however, it can be stated that the system has critical damping and this value will be applied in the model.

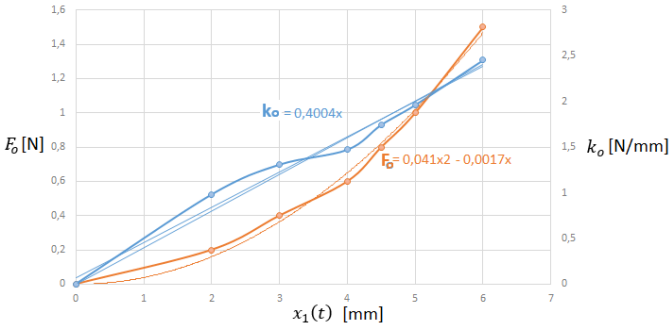

Figure 3. Experimental data from k_o measuring test

Factors k_s and c_s are modelling the foundation of the motor that can be a vibroinsulation, whose purposefulness of use will be examined later in the study. In the current structure, vibroinsulation does not occur, therefore: $k_s = 1000$ N/mm and $c_s = 0$ kg/s.

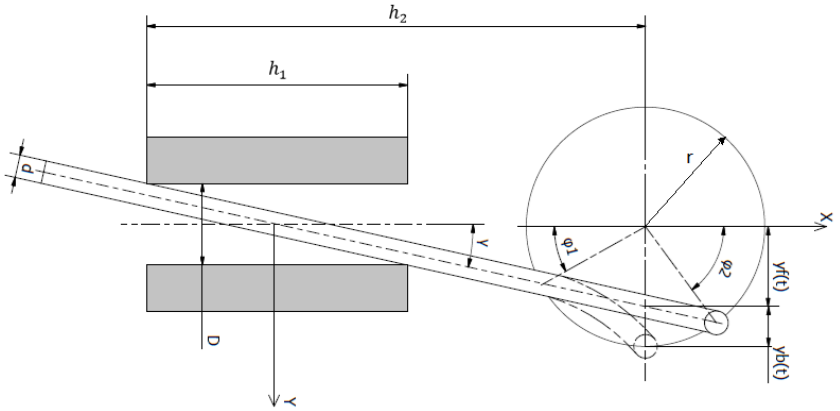

Figure 4. Needle behaviour

The element that brings energy into the system is the motor with mass $m_s = 55$ g and moment of inertia I_s. It rotates at a constant speed $\dot{\varphi} = 8000\ \frac{\pi}{30}$ rad/s and through the eccentricity $m_n = 1$ g drives the needle $m_i = 0.3$ g . Due to fact that in the mechanism connecting rod and the slider cannot distinguished, during the operation the angular position of the needle changes, and also – because of the limited radial clearance $D - d$ it is bent in a certain angular range. As a result, the stiffness of the needle is changing in the function of the angle of rotation – its value has been numerically determined in the FEM environment. For this purpose, an analysis of the condition of the needle was carried out depending on the angular position of the motor. According to Fig. 4. the limit positions of needle joint positions at which its bending begins can be determined by solving the system of equations for xp and yp:

$$\begin{cases} yp^2 + (xp - h_2 + 0.5h_1)^2 = r^2 \\ xp = yp \cdot \mathrm{tg}(Pi/2 - \gamma) \\ \gamma = \arcsin\left(D/\sqrt{D^2 + {h_1}^2}\right) - \arcsin\left(d/\sqrt{D^2 + {h_1}^2}\right) \end{cases} \tag{1}$$

The above system of equations has two pairs of solutions that correspond to the points of intersection of the axis of the needle, which is freely based on the sleeve and the point of the hang of the needle. The boundary angles are:

$$\begin{cases} \varphi g_1 = \arcsin\left(\frac{yp_2}{r}\right) \\ \varphi g_2 = \arcsin\left(\frac{yp_1}{r}\right) \end{cases} \tag{2}$$

Accordingly, the deflection of the needle $yb(t)$ is given by the equation:

$$yb(t) = \begin{cases} 0 & t \in \langle 0, \quad \frac{\varphi g_1}{\dot{\varphi}} \rangle \\ r \cdot \sin(\dot{\varphi}\, t) - yf_1(t) & t \in \left(\frac{\varphi g_1}{\dot{\varphi}}, \quad \frac{\pi - \varphi g_2}{\dot{\varphi}}\right) \\ 0 & t \in \langle \frac{\pi - \varphi g_2}{\dot{\varphi}}, \quad \frac{\pi + \varphi g_2}{\dot{\varphi}} \rangle \\ r \cdot \sin(\dot{\varphi}\, t) - yf_2(t) & t \in \left(\frac{\pi + \varphi g_2}{\dot{\varphi}}, \quad \frac{2\pi - \varphi g_1}{\dot{\varphi}}\right) \\ 0 & t \in \langle \frac{2\pi - \varphi g_1}{\dot{\varphi}}, \quad \frac{2\pi}{\dot{\varphi}} \rangle \end{cases} \tag{3}$$

The parameter $y_f(t)$ describes the equilibrium point at which the needle is bent in a specific motor position and it is described by the expression:

$$yf_i(t) = \frac{h_2 - 0.5h_1}{\pm \mathrm{tg}(\pi/2 - \gamma) - \mathrm{tg}(\pi/2 - \varphi)} \tag{4}$$

As can be seen in equation (2), for some range of φ the needle is bent. The equation of her deflection takes the form:

$$y = -\frac{yb(t)}{(h_1)^2 - (h_2)^2}x^2 + \frac{h_1 \cdot yb(t)}{(h_1)^2 - (h_2)^2}x \tag{5}$$

For the remaining angular positions, the needle remains straight but deviates from the vertical by an angle α equal to:

$$\alpha = \mathrm{arctg}\left(\frac{r \cdot \sin\varphi}{r \cdot \cos\varphi + h_2 - 0{,}5h_1}\right) \tag{6}$$

According to the above criteria, 19 needle models were prepared. They are corresponding to the subsequent positions and shapes of the needle as a function of the motor positions varying from 0 to 180° with step equal to 10° and two additional needle models at the boundary positions. In the ANSYS environment, the end of the needle that determine the connection to the eccentric was loaded with force in the direction *X* (vertical) 2 N, while the second was fixed. The displacement of the loaded needle end in the direction *X* caused by compression and buckling was examined. The stiffness coefficient was determined by dividing the value of applied force by appropriate deflection. The diagram of elasticity coefficient $k_i(\varphi(t))$ values of the needle is shown in Fig. 5.

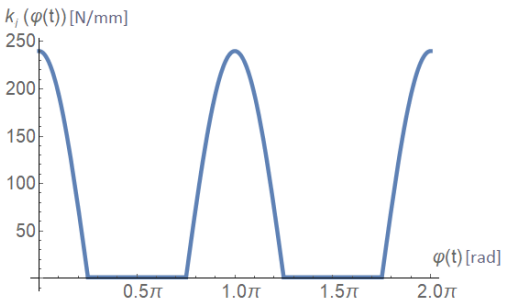

Figure 5. $k_i(\varphi(t))$ diagram

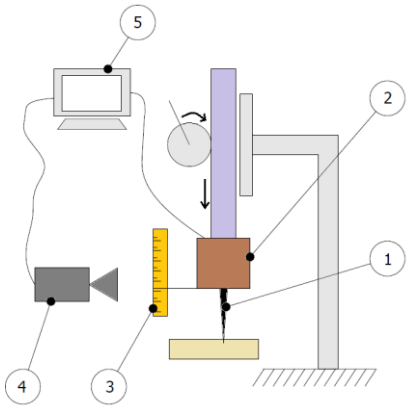

Figure 6. $k_p(\varphi(t))$ test station

The element $k_p(\varphi(t))$ is a model of the elastic interaction of the needle with the body. It was assumed that contact occurs at $\varphi = \pi/2$ rad, then the skin is stretched and the stiffness factor increases according to the data obtained experimentally. The test was carried out at the station, the diagram of which is shown in figure 6. During the test, the

indenter (6.1) coupled with the tensometer (6.2) is pressing into the skin. The size of the cavity is read from the measuring scale (6.3) by the vision system (6.4) and related to the value of current pressing force by authorial software on PC (6.5), which also converting this information on $k_p(\varphi(t))$ function.

On the basis of the dynamic simulation of the event in the ANSYS environment it was found that the yield point of the skin [7] will occur after skin deformation to a depth of 3.2 mm. which corresponds to motor angular position close to $\varphi = 3\pi/4$ rad. During skin penetration, the elasticity coefficient drops to an estimated value of 0.3 N/mm and during the retraction of the needle it drops even further to 0.2 N/mm. The plot of the change in stiffness coefficient $k_p(\varphi(t))$ is shown in the graph in Fig. 7.

The damping coefficient $c_p(\varphi(t))$ will be subject to abrupt changes, as well as the coefficient of elasticity $k_p(\varphi(t))$, thus assumed $c_p(\varphi(t)) = a\, k_p(\varphi(t))$, where $a = 0.5$. The impact of the correctness of this assumption on the results was examined in the following part of the work.

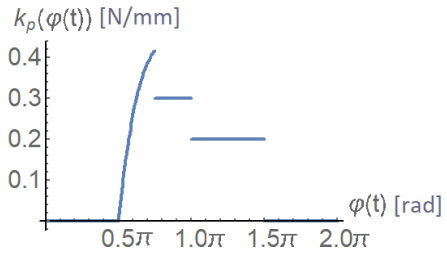

Figure 7. $k_p(\varphi(t))$ diagram

The structure is loaded with three forces: the unbalance force of the motor $P_n(\varphi(t))$ and the friction forces between the needle and the sleeve $T_2(\varphi(t))$ proportional to the deflection $z(t)$. It is worth noting that $P_n(\varphi(t)) >> T_i(\varphi(t))$, thus the impact of the adopted value of the coefficient of friction $\mu = 0.1$ will have a marginal significance on the obtained results. Coordinates of points of application of each force depend linearly on $x_1(t)$, moreover $P_n(\varphi(t))$ depends also on $x_2(t)$, hence it can be written: $Q_1(t) = P_n(t) + T_1(t) + T_2(t)$, $Q_2(t) = P_n(t)$, $Q_3(t) = 0$. The equations of motion of the system then take the form:

$$\begin{aligned} M\ddot{x}_1(t) + (c_o + c_s)\dot{x}_1(t) - c_s\,\dot{x}_2(t) + (k_o + k_s)x_1(t) - k_s\,x_2(t) &= Q_1(t) \\ m_s\ddot{x}_2(t) + (c_i + c_s)\dot{x}_2(t) - c_s\,\dot{x}_1(t) - c_i\,\dot{x}_3(t) + (k_i + k_s)x_2(t) & \\ -k_s\,x_1(t) - k_i\,x_3(t) &= Q_2(t) \\ m_i\ddot{x}_3(t) + (c_i + c_p)\dot{x}_3(t) - c_i\,\dot{x}_2(t) + (k_i + k_p)x_3(t) - k_i x_2(t) &= 0 \end{aligned} \tag{7}$$

The above system of equations was solved numerically in the Wolfram Mathematica environment, for zero initial conditions and nominal angular velocity $\dot{\varphi} = 838$ rad/s (8000 rpm).

3. Results

Displacement graphs and phase diagrams for each degree of freedom are presented in Fig. 8 and Fig. 9.

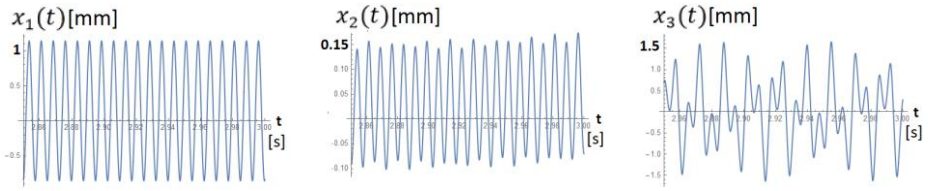

Figure 8. Displacement graphs

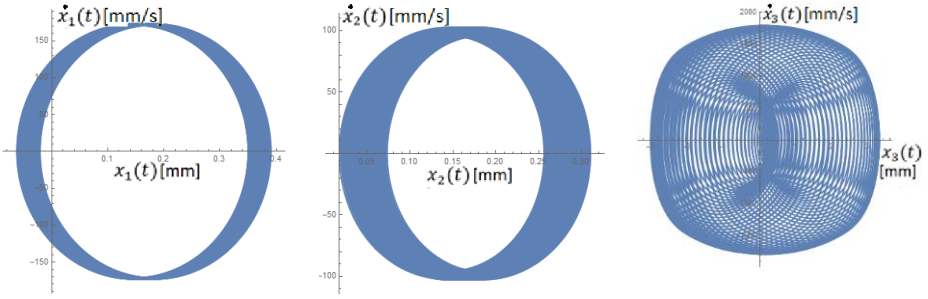

Figure 9. Phase diagrams

As the graphs shows, during operation of the machine there a vibrations with a relatively large amplitude occur. According to the model, the foundation of the motor can be a vibration isolation that minimizes vibrations transmitted to the body. The condition of vibroinsulation, apart from the possibly high damping ratio is:

$$k_s < \frac{\dot{\varphi}^2 M}{9} = 2.5\ \mathrm{N/mm} \tag{8}$$

Both these conditions are meet up by a rubber sleeve with external diameter $D_s = 8\ \mathrm{mm}$, internal diameter $d_s = 6\ \mathrm{mm}$ and height $h = 14\ \mathrm{mm}$, for which $k_s = 2.4\ \mathrm{N/mm}$ and $c_s = 0.028\ \mathrm{kg/s}$. Such sleeve – after modification of the body – can be placed as an medial element between the motor and the body. The graphs presented in Fig. 10 indicate that such procedure is the highly reasonable – amplitude of the body vibrations dropped almost five times. This is accompanied by more than threefold increase in the amplitude of the motor, which is also a desirable phenomenon – these vibrations are shifted in phase with the needle's vibrations for almost half a period, so they will partially compensate the uncontrolled swinging of the needle, thereby increasing comfort and quality of work.

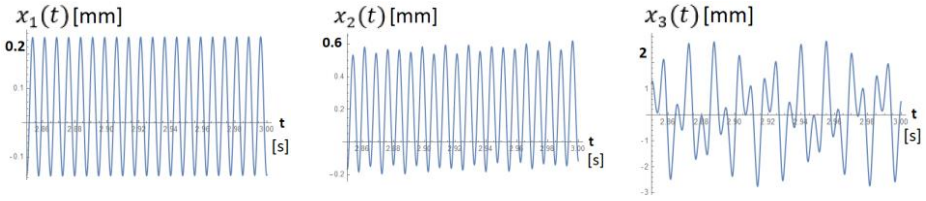

Figure 10. Vibration amplitudes of vibroinsulated motor

The accuracy of the results could be questioned due to numerous parameters values have been roughly adopted or their value is strongly individualized. Among these parameters (c_o, c_p, k_p, a, μ) only the value of c_o coefficient had a significant impact on the amplitude of body vibrations – in the parameter range from 0 to 10˚, an input amplitude (without vibroinsulation) decreased by 28% but only by 13% in relation to adopted critical damping $c_o = 5\,\mathrm{kg/s}$. This parameter could be controlled by modification of dynamical parameters of rubber spacer (1.5). Moreover, it should be mentioned that the strong nonlinearity of the k_p coefficient causes vibrations to take place around the non-equilibrium position, but the values adopted in the model do not significantly affect this effect or the behavior of the system.

4. Conclusions

The work is analysis of the dynamics of the tattoo device model with three degrees of freedom. The elastic properties that describe the interaction of the device with the operator were determined by numerical simulations using the finite element method. It showed the relation between the stiffness coefficient and the shift from the equilibrium position of the device's body. Simulation tests of the stiffness factor of the needle showed strongly nonlinear dependence of this parameter on the angular position of the machine's motor. Due to the cyclical gap between the skin of the tattooed person and the needle, the model describing this interaction showed strong nonlinearity and, in addition, the nonlinearity increased by the hyperelastic properties of the skin. The inertia load of the system and the nonlinear friction forces occurring in it were determined analytically. Due to the fact that the remaining part of the parameters has been estimated, analyzes have been carried out to examine how the values of these parameters affect the maximum value of the amplitude of the body vibrations. They revealed that only the increase in skin damping coefficient significantly reduced vibrations. The work also contains an proposition of effective vibroisolation of the system, which allows for a nearly fivefold reduction of body vibrations.

References

1. K. J. Leader, *Occupy your Body: Activating 21st–Century Tattoo Culture*, The Journal of Somaesthetics, **3** (2017) 44 – 57.
2. L. Krutak, *The cultural heritage of tattooing: A brief history*, Current problems in dermatology **48** (2013) 1 – 5.

3. *Technology Takes Tattoos into the Future*, [open access: https://www.asme.org/engineering-topics/articles/design/technology-takes-tattoos-into-future].
4. N. Kluger, *National survey of health in the tattoo industry: Observational study of 448 French tattooists*, International Journal of Occupational Medicine and Environmental Health, (2017) 111 – 120.
5. J. Łuczko, *Drgania nieliniowe i chaotyczne w nieliniowych układach mechanicznych*, Politechnika Krakowska, Kraków, 2008.
6. [http://www.tommyssupplies.com/66308/794444/Legend-Rotary/Legend-Rotary-Black.html].
7. H. Chaudhry, B. Bukiet, *Deformations Experienced in the human skin, adipose tissue, and fascia in osteopathic manipulative medicine*, The Journal of the American Osteopathic Association, (2014) 780 – 787.
8. T. Irvine, *Damping properties of materials*, [open acces: https://syont.files.wordpress.com/2007/05/damping-properties-of-materials.pdf].